Bending of DNA by the Mitomycin C-Induced, GpG Intrastrand Cross-Link

Stacia M. Rink, Roselyn Lipman, Stephen C. Alley, Paul B. Hopkins,* and Maria Tomasz*

Department of Chemistry, Hunter College, City University of New York, New York, New York 10021, and Department of Chemistry, University of Washington, Seattle, Washington 98195

Received September 7, 1995[⊗]

Mitomycin C (MC) forms interstrand and intrastrand cross-link adducts and monoalkylation products (monoadducts) with DNA. Each of the three types of adducts was incorporated site-specifically into both a 15-mer and a 21-mer oligodeoxyribonucleotide duplex. The adduct-containing duplexes were ^{32}P-phosphorylated and ligated to form multimers, which were then analyzed for anomalous electrophoretic mobility by nondenaturing polyacrylamide gel electrophoresis, using the method of Koo and Crothers [(1988) *Proc. Natl. Acad. Sci. U.S.A.* **85**, 1763−1767] in order to detect DNA curvature caused by the adducts. The intrastrand cross-link adduct was found to induce a 14.6 ± 2.0° DNA bend per lesion (minimum value) while no DNA bending was detected for either the interstrand cross-link or the monoadduct. Molecular mechanics modeling indicated that the possible origin of the bend lies in a considerable deviation from parallel of the normals to the best planes of the intrastrand cross-linked guanines, due to a shorter than normal distance between their N^2 atoms forced upon them by the cross-link. The observed bending by the MC intrastrand lesion may be the cause of the increased flexibility of MC-modified DNA, localized to distinct regions, as observed in earlier work by hydrodynamic methods and electron microscopy. The MC adduct-caused DNA bend may serve as a recognition site for certain DNA-binding proteins.

Introduction

The natural product mitomycin C (MC;[1] **1**), produced by the mold *Streptomyces caespitosus*, possesses antitumor and antibiotic properties and is used extensively in cancer chemotherapy. Its biological activity is fundamentally related to its propensity to bind covalently to DNA and cross-link the complementary strands. (For a review and references, see ref 1.) The mitomycins represent the prototype of natural products capable of inducing a DNA cross-link,[2] one of the most lethal types of DNA lesions. The chemical structure of the MC cross-link has been elucidated as the bisguanine−MC adduct **4** (*4*). In addition, three other major covalent guanine−MC adducts were isolated and identified from DNA: two closely related monoadducts **2** (*5*) and **3** (*6*) and the bisadduct **5** (*7*), the latter corresponding to a DNA *intrastrand* cross-link. The same major MC adducts were shown to be formed in tumor cells (*8*) and in rat liver (*4*). The structures indicated that the reaction of MC with DNA is exquisitely specific: both the C1-aziridine and the C10-carbamate alkylating functions of the drug react exclusively with 2-amino groups of guanines, in the minor groove of DNA. Furthermore, the reaction is specific to *DNA sequence*: MC alkylates guanines in the CpG·CpG sequence approximately 10 times faster than guanines in other sequence contexts (*9*−*11*). This monoalkylation selectivity coincides with the observed spatial restriction of interstrand cross-link formation to the same CpG·CpG site (*12*−*14*). Thus the structure of MC may be thought to have been "optimized" by molecular evolution to work as an interstrand bifunctional cross-linking agent: it recognizes and alkylates guanines preferentially in the CpG·CpG sequence, wherein it can be converted subsequently to a cross-link (*10*).

Recent studies of various covalent drug−DNA complexes have led to new concepts of how a covalent DNA lesion might inhibit DNA function. Notably, several drugs have been shown to cause bending of the helix axis of duplex DNA due to local distortion by the adduct (*15*−*23*), and in some cases this was shown to correlate with altered affinity to DNA-binding proteins. In particular, intrastrand cross-link adducts of cisplatin (*24, 25*) and the major adduct of *anti*-benzo[*a*]pyrene diol epoxide (BPDE) (*26*) both bend DNA and induce "illegitimate" binding of transcription factors at the adducted DNA site. In both cases, the binding was specific to certain adducts within the multiple DNA adduct spectrum of the drugs. In contrast, the drug CC-1065, which both alkylates and bends AT-rich segments of DNA, abolished the binding affinities of certain DNA-binding proteins at their binding site (*27*).

So far the DNA adducts of MC have not been investigated for their ability to alter global DNA structure, as by bending, for example. The reaction of MC with DNA exhibits a multiple-adduct spectrum (Scheme 1), similar to the case of cisplatin and BPDE. While attention usually has been focused on the interstrand cross-link **4** as the biologically most significant lesion caused by MC, there are indications that some of the other adducts are also cytotoxic (*28*) and inhibit DNA template functions in cell-free systems (*29*). In order to further our understanding of structure−activity relationships of the MC adducts, we examined and compared the DNA-bending ability of the three major species (Chart 1), monoadduct

⊗ Abstract published in *Advance ACS Abstracts,* January 1, 1996.

[1] Abbreviations: MC, mitomycin C; BPDE, (±)-7*r*,8*t*-dihydroxy-9*t*,-10*t*-oxy-7,8,9,10-tetrahydrobenzo[*a*]pyrene; TEAA, triethylammonium acetate; R_L, relative mobility.

[2] Carzinophilin, the only other natural antibiotic noted for DNA cross-linking activity, has not yet been fully characterized structurally (*2, 3*).

0893-228x/96/2709-0382$12.00/0

Scheme 1

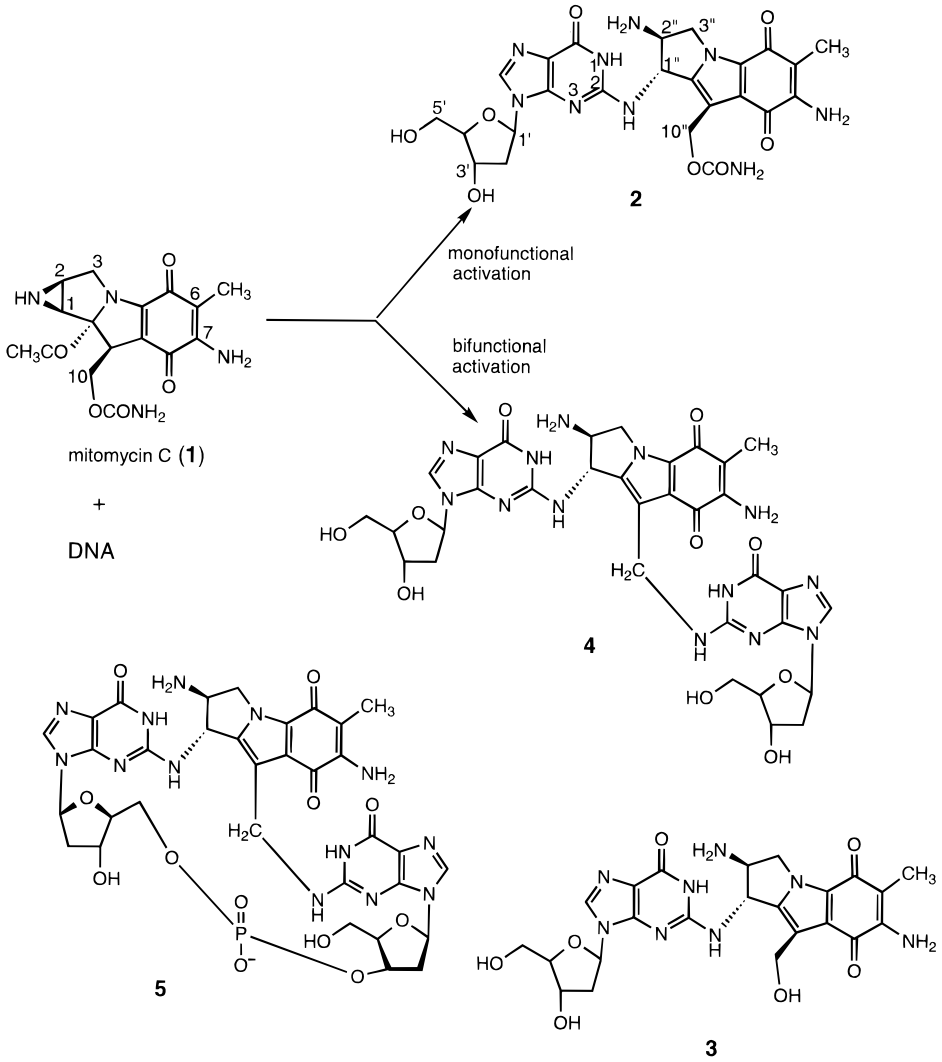

Chart 1

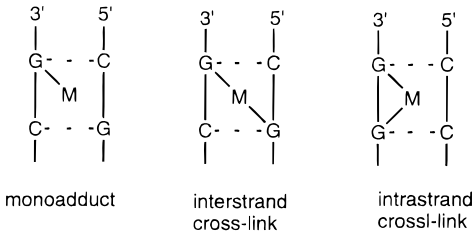

3, interstrand cross-link adduct **4**, and the intrastrand cross-link adduct **5**, by the method of electrophoretic mobility shifts of ligated oligomers containing site-specific adducts (*30*). We report that the intrastrand cross-link selectively induces bending of duplex B-DNA, while the monoadduct and interstrand cross-link have no effect on DNA global structure.

Experimental Section

Materials and Methods. Mitomycin C was obtained from Bristol-Myers Squibb Co. (Wallingford, CT). Synthetic oligodeoxyribonucleotides were prepared on an Applied Biosystems Model 38013 DNA synthesizer using the cyanoethyl phosphoramidite method. The "trityl-off" preparations were deprotected according to standard protocol and desalted by passing through a Sephadex G-25 (fine) column using 0.02 M NH_4HCO_3 as eluant, followed by lyophilization. Ligation and electrophoresis protocols were as described previously (*31*), except: T4 DNA ligase was obtained from Amersham (Arlington Heights, IL) and ATP from Aldrich (Milwaukee, WI). The plasmid pBR322 and *Hin*fI and *Hae*III restriction enzymes were obtained from New England Biolabs (Beverly, MA). Nondenaturing loading buffer consisted of 30% (aq) glycerol, 0.25% bromophenol blue, and 0.25% xylene cyanol dyes. One unit of T4 DNA ligase is defined as the amount of enzyme required to convert 1.0 nmol of ^{32}P from pyrophosphate into Norit-adsorbable form in 20 min at 37 °C. OD refers to the calculated absorbance at 260 nm of the sample in 1 mL of solvent in a 1 cm path length cell. The extinction coefficients at 260 nm for DNAs were estimated to be 10 000 M^{-1} cm^{-1} $residue^{-1}$.

Synthesis and Purification of Oligonucleotides Containing Site-Specific Mitomycin Adducts. (i) Interstrand Cross-Link Adduct (4) Series. The "two-step" method was employed, as described in detail for other mitomycin-cross-linked oligonucleotides in a previous publication (*32*). Specifically, the top strands of **7** and **9** (160 and 240 OD units, respectively) were each annealed with the 8-mer template, 5′-ATAm^{5}CGTGA (1 mol strand equivalent), and then submitted to monoalkylating conditions by MC (0.5 mol equivalent of $Na_2S_2O_4$ per mole of MC) in 0.1 M sodium phosphate, pH 7.5 buffer under aerobic conditions at 0 °C, 1 h reaction time. The monoalkylated top strands of **7** and **9** were isolated from the reaction mixtures by preparative HPLC using a 2.14 × 25 cm C-4 reversed phase column (Rainin, Dynamax) and a gradient of 6−10.5% acetonitrile in 0.1 M triethylammonium acetate (TEAA) buffer, pH 7.0, in 10 min, at a flow rate of 10 mL/min. The desalted monoalkylated oligonucleotides were each an-

nealed with the corresponding complementary bottom strands of **7** and **9** and treated with excess $Na_2S_2O_4$ under anaerobic conditions at 0 °C. The resulting cross-linked duplexes **8** and **10** were isolated by Sephadex G-50 (5 × 56 cm) column chromatography; each eluted earlier (150 mL) than non-cross-linked material (240 mL). The overall yields, based on **7** and **9**, were 12% and 17%, respectively.

(ii) Intrastrand Cross-Link Adduct (5) Series. These syntheses were carried out in one step, as described in detail previously, for various oligonucleotides (*7*). Specifically, the top strands of **11** and **13** (160 and 200 OD units, respectively) were each annealed with the 8-mer template 5′-ATAm^{5}CCTGA (1 mol strand equivalent) and submitted to bifunctional alkylating conditions (anaerobic, excess $Na_2S_2O_4$). The resulting intrastrand cross-linked top strands of **12** and **14** were isolated by preparative HPLC (same system as above), in 3.8% and 3.2% yields, respectively, based on OD units of the starting parent strands.

(iii) Monoadduct (3) Series. Only the 21-mer was prepared in this series. Specifically, the monoadduct-substituted top strand of **15** was isolated from the same reaction, which yielded the intrastrand cross-link-substituted product (top strand of **14**, see above). Its yield, after isolation by HPLC, was 2.5% based on the OD units of the starting parent strand. All adducts were subsequently purified by denaturing gel electrophoresis.

Characterization of Adduct-Substituted Oligonucleotides. Locating the desired compounds in specific HPLC peaks upon chromatography of the reaction mixtures was accomplished by analysis of an aliquot of each collected 320 nm-absorbing peak as follows: Enzymatic digestion to individual nucleosides and adducts was employed, followed by identification of the adducts *via* HPLC coelution with authentic standard adducts **3**, **4**, and **5**, using previously described methods (*4, 5*). Quantitative nucleoside composition was also determined to verify the structures (*14*); satisfactory analysis was obtained in all cases.

Ligation. The non-cross-linked, monoadducted, and cross-linked duplexes (0.2 OD 20-mer, 0.3 OD 15-mer) and a *Bam*HI linker duplex ([5′-d(CGGGATCCCG)]$_2$, 0.4 OD) were independently phosphorylated at their 5′-ends with [γ-^{32}P]ATP (20 μCi) using T4 kinase (16 units) in kinase buffer (10 μL final volume). The samples were incubated at 37 °C for 0.5 h, followed by the addition of cold ATP (0.5 μL of 5 μM stock solution), T4 kinase (8−16 units), and kinase buffer for a final volume of 20 μL. After gently mixing, the samples were incubated for 1.0 h at 37 °C.

T4 DNA ligase (8 units for non-cross-linked duplexes, 12 units for cross-linked and *Bam*HI) and ATP (2.5 mM final concentration) were added directly to the phosphorylated duplex samples. After mixing, the samples were incubated at 10−12 °C for 15 h. An additional 12 units of ligase was added to each sample, and the samples were incubated for another 15 h at 10−12 °C. Absolute ethanol (1 mL, −20 °C) was added to a portion (3−5 μL) of each ligation reaction, the ligation products were collected by centrifugation, and the recovered material was washed once with 1 mL of a cold (−20 °C), 85% (aq) ethanol solution. The samples were dried *in vacuo* at 25 °C and then admixed with 10 μL of nondenaturing buffer.

Size Marker Preparation. Length markers were prepared by digestion of 5 μg of pBR322 DNA in the presence of 1 unit of *Hae*III or *Hin*fI restriction enzyme at 37 °C for 3 h. The buffer conditions were 100 mM NaCl, 10 mM Tris-HCl (pH 8.0), 10 mM $MgCl_2$, and 0.5 μg/10 μL BSA. A portion (0.16−0.35 μg) of each digest (1 μL) was taken up in kinase buffer and phosphorylated with [γ-^{32}P]ATP using T4 kinase (16 units) at 37 °C for 0.5 h in the presence of 1 mM ADP. An equal volume of loading buffer was added to the reaction, and one-fourth of this mixture was used in each marker lane on a native gel.

Electrophoresis. Electrophoresis was performed using a nondenaturing 8% polyacrylamide gel (mono:bis-acrylamide ratio 29:1). The gels were polymerized for 1 h and prior to loading samples were run in TBE buffer (1 × TBE, pH 8.3) for 1 h at 2 °C with a constant voltage of 1000 V. After loading the samples, the gel was run at a constant voltage of 1000 V until the xylene cyanol dye had migrated 22−24 cm. The gels were dried under vacuum for 15 min at 80 °C, to prevent band diffusion, and subsequently analyzed by autoradiography and phosphorimagery.

Calculation of Band Mobilities. The electrophoretic mobility of a given band was assigned as the maximum in a densitometric plot derived from the phosphorimage of ligation ladder gels. Mobilities were converted to relative length, R_L, as described by Koo and Crothers (*33*):

$$R_L = L_a/L_r$$

where L_a is the apparent length of the multimer, as described by the size (in bp) of the *Bam*HI multimer whose mobility corresponds to the multimer of interest, and L_r is the real length of the multimer of interest (in bp). The angle of absolute curvature per turn of DNA, C, for selected multimers was estimated following the empirical relation of Koo and Crothers (*33*):

$$C = [(R_L - 1)/((9.6 \times 10^{-5})L_a{}^2 - 0.47\ \text{bp}^2)]^{1/2} \times (19.75 \pm 2.75\ \text{deg bp turn}^{-1})$$

The length of a DNA present in a given band of the *Bam*HI ligation ladder was assigned based upon comparison of its mobility relative to a corresponding DNA size marker. The size markers were generated as described previously.

Computation. Computations were performed on a Silicon Graphics Iris Indigo XS-24 work station utilizing the Builder, Biopolymer, and Discover (v. 2.9) modules of Insight II (v. 2.2.0) (Biosym Technologies, San Diego, CA). Energy minimizations were performed with the AMBER forcefield, a distance-dependent dielectric of 1.0*r in the absence of solvent and counterions, a nonbonded cutoff of 12 Å, and no Morse or cross terms. The starting structures were the B-like DNA duplexes 5′-d(AGGT)·5′-d(ACCT) (intrastrand) and [5′-d(ACGT)]$_2$ (interstrand). The cross-links were formed by visually docking the mitosene into the middle of the minor groove and forming bonds to the N^2 atoms of the cross-linked guanines. All hydrogen bond lengths and the terminal glycosyl torsion angles were constrained to keep the short duplexes annealed and the backbone conformation B-like during the minimization. Structures were minimized by the method of steepest descents for 300 iterations followed by the method of conjugate gradients until the maximum derivative for any atom was less than 0.01 kcal/(mol·Å) (requiring 1000−3000 iterations). The terminal base pairs were then removed and the remaining structures were extended into the B-like DNA duplexes 5′-d(TTCAGGTATG)·5′-d(CATACCTGAA) (intrastrand) and 5′-d(TTCACGTATG)·5′-d(CATACGTGAA) (interstrand). These structures were energy minimized as above. Finally, the C1″/C10″−N^2−C2−N1/N3 guanine and H−N^4−C4−N3/C5 cytosine torsions were constrained to place the C1″/C10″−N^2 and H−N^4 bonds in the plane of the attached bases and energy minimized as above. Helix structures were evaluated using the program Newhelix 91, kindly provided by Professor Richard Dickerson, University of California at Los Angeles.

Results

Design and Synthesis of MC−Oligonucleotide Complexes (Charts 1 and 2). A 15-mer and a 21-mer duplex series were designed, both of which had complementary 5′-terminal, one-nucleotide overhangs, for the purpose of self-ligation in a later step. A central CpG·CpG sequence was targeted for interstrand cross-links (**8**, **10**), and a central GpG·CpC sequence was targeted for both intrastrand cross-links and monoadducts (**12**, **14**, and **15**, respectively).

MC reacted directly with the designated target guanines under reductive activating conditions. To ensure selectivity to only the targeted guanine, a shorter tem-

Chart 2. Structures of Parent and Mitomycin-Substituted Oligonucleotides

Interstrand cross-link series

15-mers: 5'-AAGTTCACGTATGCC
3'-TCAAGTGCATACGGT

7 (parent)

5'-AAGTTCACGTATGCC
M
3'-TCAAGTGCATACGGT

8

21-mers: 5'-AGTAAGTTCACGTATGCCATT
3'-CATTCAAGTGCATACGGTAAT

9 (parent)

5'-AGTAAGTTCACGTATGCCATT
M M = as above
3'-CATTCAAGTGCATACGGTAAT

10

Intrastrand cross-link series

15-mers: 5'-AAGTTCAGGTATGCC
3'-TCAAGTCCATACGGT

11 (parent)

M
5'-AAGTTCAGGTATGCC
3'-TCAAGTCCATACGGT M = as above

12

21-mers: 5'-AGTAAGTTCAGGTATGCCATT
3'-CATTCAAGTCCATACGGTAAT

13 (parent)

M
5'-AGTAAGTTCAGGTATGCCATT
3'-CATTCAAGTCCATACGGTAAT

14

Monoadduct Series

21-mers: **13** (parent)

M
5'-AGTAAGTTCAGGTATGCCATT
3'-CATTCAAGTCCATACGGTAAT

15

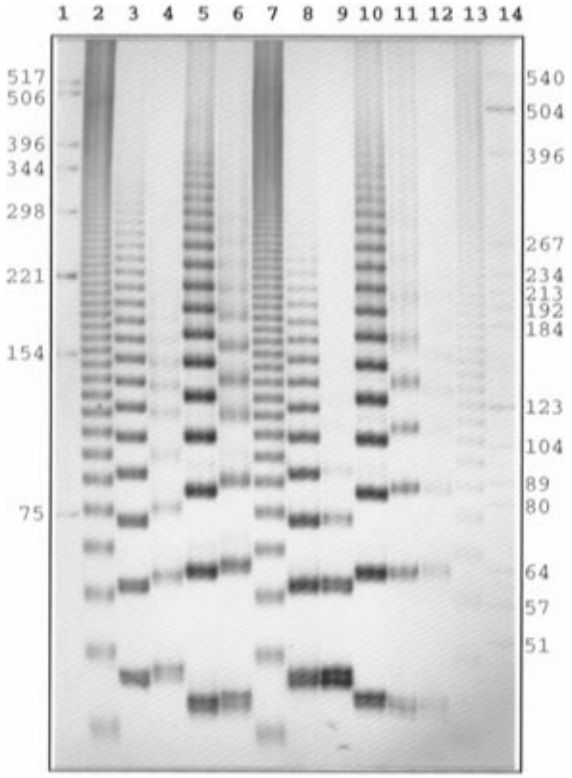

Figure 1. Autoradiogram of ligation ladder. Lane 1: *Hin*fI digest of pBR322; lanes 2, 7, 13: *Bam*HI linker; lanes 3−6: native and interstrand cross-linked DNAs **7**, **8**, **9**, and **10**, respectively; lanes 8−11: native and intrastrand cross-linked DNAs **11**, **12**, **13**, and **14**, respectively; lane 12: monoadducted DNA **15**; lane 14: *Hae*III digest of pBR322. Numbers on the left and right sides of the autoradiogram correspond to the lengths of the fragments produced by the *Hin*fI and *Hae*III digests of pBR322, respectively. The origin of the band broadening and/or doubling observed in all ligated products was not investigated.

plate, complementary to the 8-mer midsegment of the oligonucleotide strand to be alkylated, was annealed to the latter. This left the *nontargeted* guanines of the oligonucleotide in the single-stranded state during the alkylation reaction, which rendered them nonreactive (*10*). In the case of **12**, **14**, and **15** the desired alkylated oligonucleotides were isolated by HPLC, further purified, and reannealed with the appropriate partner strands for the self-ligation step. The interstrand cross-link series (**8** and **10**) was prepared somewhat differently: After the templated monoalkylation step above, the purified monoadduct-containing 15-mer or 21-mer strand was converted in a second step to the final cross-linked duplexes **8** and **10**, respectively. This two-step procedure of cross-linking avoided the formation of *two cross-link orientation isomers* which are usually hard to separate and distinguish (*32*).

All of the DNAs in Chart 2, as well as a *Bam*HI linker (size marker), were exhaustively phosphorylated using T4 kinase and [γ-^{32}P]ATP. The resulting products were ligated using T4 ligase and analyzed by nondenaturing PAGE (mono:bis-acrylamide ratio 29:1) as shown in Figure 1. The mobilities observed for the ligated multimers were converted to relative mobilities (R_L) by reference to the multimers from the *Bam*HI linker. The lengths of the products of *Bam*HI ligation were assigned by comparison to size standards generated by *Hae*III/pBR322 and *Hin*fI/pBR322 digests. The resulting values were plotted versus multimer length.

Multimers of the parent duplexes (**7**, **9**, **11**, **13**) showed no anomalies in electrophoretic mobility, the R_L values at all lengths showing no significant deviation from 1.0 (Figure 2). This indicated that these DNAs all possessed unbent helix axes. The situation was little different for the cases of the interstrand cross-linked 15-mer (**8**) and 21-mer (**10**) as well as the monoadducted DNA (**15**). In these cases, multimers up to ca. 160 bp in length showed little to no electrophoretic anomaly, with R_L values below 1.13 in all cases. For comparison, phased multimers

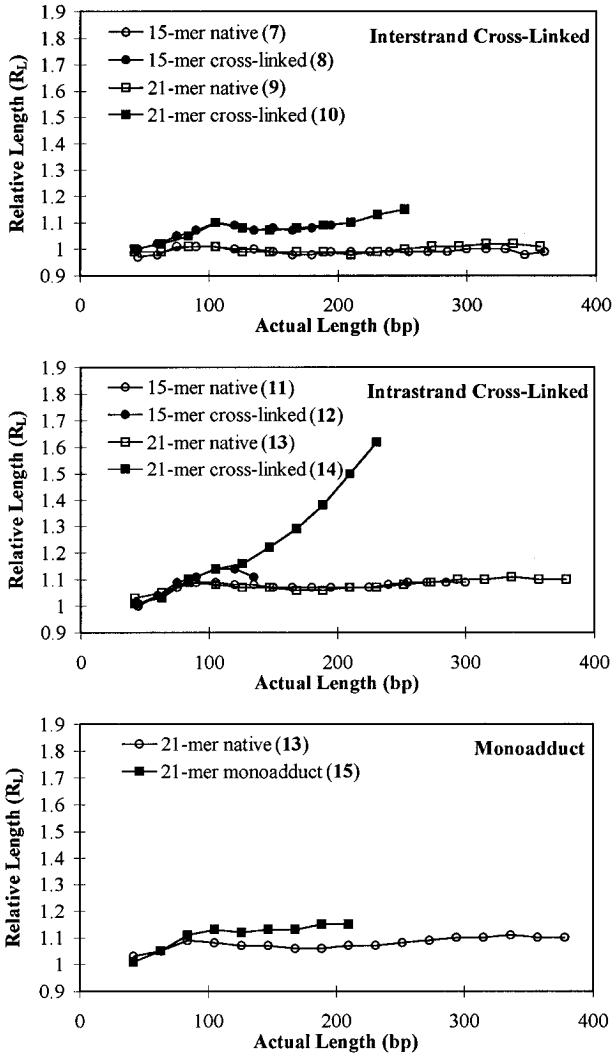

Figure 2. Relative length of mitomycin-modified DNAs as a function of actual length.

containing a bent AT tract have shown R_L values in excess of 2.0 at this length (*34*). The interstrand cross-link and monoadduct thus appear not to bend the DNA helix axis.

The situation with the intrastrand cross-linked DNA was entirely distinct. The electrophoretic mobilities of multimers of the intrastrand cross-linked 21-mer (**14**) were significantly retarded, and the anomaly increased with length. The longest multimer whose mobility could be reliably determined displayed an R_L of 1.5 (210 bp in length). This is the behavior expected for a lesion which minimally reorganizes DNA with regard to torsional organization, but introduces a bend into the helix axis. The 21-residue repeat (2.0 turns of B-DNA) thus brings these bends into phase, creating a net planar curvature. The behavior of the intrastrand cross-linked 15-mer (ca. 1.5 turns of B-DNA) was thus of great interest, having the potential to distinguish whether intrastrand cross-linking introduces a statically bent structure or anisotropic joint, as opposed to a universal or hinge joint. Although the intrastrand cross-linked 15-mer (**12**) did not ligate with high efficiency, providing a multimer of length 135 bp as the largest band which could be reliably located, we interpret the data (Figure 2) as preliminary evidence against a universal or isotropic hinge joint. Rather, the intrastrand cross-link is a statically bent structure or an anisotropic joint.

The extent of curvature for the intrastrand cross-link was calculated using the empirical relationship of Koo and Crothers (*33*). The intrastrand cross-link 21-mer (**14**) was found to be bent by 14.6 ± 2.0° per cross-link at 147 bp. Because we did not optimize the intrastrand cross-link spacing by varying the length of the ligated multimers (e.g., 17, 19, 21, 23, 25, etc.), this value should be considered a lower limit. The 15-mer intrastrand cross-link, the interstrand cross-links, the monoadducts, and the native DNAs were not amenable to analysis with this formula because the observed R_L values were all below the cutoff (R_L 1.2) for multimers 120−170 bp in length. The extent of curvature must therefore be less than 11.6 ± 1.6° per 2 turns (or per one lesion) for the 21-mers or 7.8 ± 1.2° per 1.5 turns (or per one lesion) for the 15-mers, which would correspond to $R_L = 1.20$.

To gain insight into the origin of the bend in the intrastrand cross-link, both mitomycin intra- and interstrand cross-links were modeled using molecular mechanics energy minimization calculations. A 4-base pair duplex was chosen as the starting point for energy minimization calculations: 5′-d(ACGT)·5′-d(ACGT) for interstrand and 5′-d(AGGT)·5′-d(ACCT) for intrastrand cross-links. For both models, the mitosene was docked in the minor groove and bonded to the N^2 atoms of the cross-linked guanines. To prevent the two strands of the duplex from dissociating during the minimization, bond length constraints were placed on the atom pairs involved in hydrogen bonding and the glycosyl torsion angles of the terminal base pairs were constrained to the value found in the starting B-like DNA structure.

Following energy minimization, the cross-linked tetramer duplexes were ligated into the center of a 10-base pair, B-like DNA: the backbone of the cross-linked duplex was superimposed onto the backbone of the B-like DNA duplex, the appropriate atoms were removed, and the appropriate bonds formed. The bond length and torsion angle constraints were released, and the structures were again energy minimized. Visual inspection of the final structure showed that the C1″/C10″-to-guanine-N^2 bonds and the cytosine-N^4−H bonds were not in the plane of the base rings, the result of a deficiency in the version of AMBER we employed (*35*). We restrained the appropriate torsions to have these bonds in the base planes, and the structures were again energy minimized.

Both the inter- and intrastrand cross-linked structures were visibly distorted around the site of the lesion, as well as appearing to be globally bent (Figure 3). Structural properties which are the result of long range, low force constant deformations, such as bending of the helix axis, are unreliably modeled by these calculations (*36*). We inspected instead the structural features which presumably result from high force constant deformations involving bond lengths and angles around the site of the lesion to understand what local forces might be involved in bending (Figure 3).

Analysis of the computed structures with the program Newhelix 91 revealed that the cross-linked guanines in the intrastrand structure were tipped (rotation about the long axis) and inclined (rotation about the short axis) (Figure 3, upper), while they were only inclined in the interstrand structure (Figure 3, lower). These changes presumably reflect the need to reduce the normal N^2−N^2 distance between the two guanines (3.6 Å at CpG·CpG and 4.3 Å at GpG·CpC), in order to match the C1″-C10″ span of the mitosene residue (3.4 Å). It is obvious that substantially more reorganization is required to

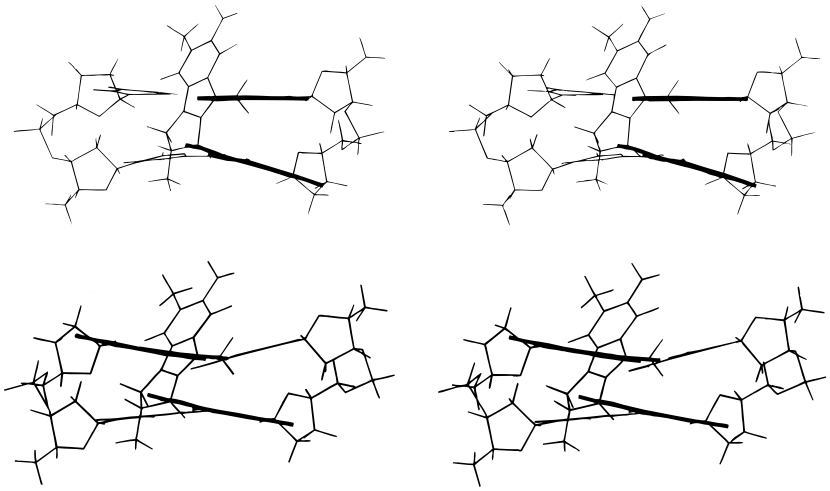

Figure 3. Stereoviews of calculated intrastrand (upper) and interstrand (lower) cross-linked DNA structures. The dinucleotide duplexes illustrated are the central portions of the energy minimized dodecamer duplexes, i.e., the cross-linked GpG·CpC and cross-linked CpG·CpG sequences, respectively. The cross-linked guanines are shown edge on in bold.

accommodate the intrastrand cross-link (GpG·CpC) sequence than the interstrand cross-link. Importantly, the normals to the best plane of the two cross-linked guanines were nearly *parallel* in the interstrand structure, but they deviated from being parallel in the intrastrand cross-link. These kinds of distortions (twist, tip, inclination) can be made manifest in a global bend if propagated by base stacking. The planes of the cross-linked guanines in the interstrand cross-linked isomer were approximately parallel to one another. No bending of the helix axis would be expected if the relative orientation of the interstrand cross-linked guanines were to be propagated by base stacking.

Discussion

The DNA−DNA intrastrand cross-link (as in **5**) induced by reductively activated mitomycin C is thus found to impart a net bend to the helix axis of duplex DNA. The corresponding monoadduct (**3**) and interstrand cross-link (**4**) either do not bend the helix axis or do so sufficiently modestly to prevent detection by the gel methods employed herein. The structural origin of the observed bending is not obvious given our current level of understanding of the DNA structure at these lesions. Although the structures of both the interstrand cross-linked and monoalkylated DNA have been studied in solution by a combination of NMR and computation (*37, 38*), these methods are at present unreliable in their predictions concerning long-range structural features such as DNA bending. The same is true of purely computational methods which have been employed to study all of these structures (*7, 39−42*).

We attempted to gain insight into the structural origin of the bend induced by the intrastrand cross-link using computation, but with a focus on the highly localized impact on the geometry of the cross-linked base pairs. We propose that the bend may result from a propagation through base−base stacking of a kink at the cross-linked GG step. This kink appears to result from the reduction in interatomic spacing of the cross-linked N^2 atoms of the cross-linked bases from the 4.3 Å separation in B-DNA to the 3.3 Å spacing observed by the cross-link. The present finding that the *monoadduct* **3** does not cause bending of the same oligonucleotide (**13**) argues well for this: The covalent structure of **13** differs from **12** only in that the second guanine is not connected to the mitosene residue; therefore, this constraint is lacking. The case of the interstrand cross-link is interesting in that it does contain the constraint of a cross-link, but is not appreciably bent. Two factors may be important in this regard: The interstrand cross-link is likely to cause less distortion than the intrastrand one, because in canonical B-DNA the N^2-to-N^2 distance between guanines on opposite strands is only 3.6 Å and therefore the DNA structure should be less distorted upon formation of a 3.3 Å-long interstrand cross-link. Furthermore, in the structures computed herein as well as elsewhere (*7, 39−42*) and in the NMR-based model (*37*), the planes of the cross-linked guanines remain essentially parallel to one another. To the extent that stacking of succeeding residues on these guanines is important in defining the path of the helix axis, this deformation could not yield a net bend. More refined understanding of the causes of the bending by the MC intrastrand cross-link must await further experimental results.

The observation of a DNA bending effect by the MC intrastrand cross-link adduct **5** adds renewed interest to our earlier finding (*43*) that MC-modified calf thymus and *Escherichia coli* DNAs displayed increased flexibility as shown by using a variety of physicochemical techniques, among them linear flow dichroism, viscosity, gel electrophoresis, sedimentation velocity, and electron microscopy. Particularly striking was the appearance of highly coiled, looped, entangled structures in the electron microscope, in contrast to control unmodified DNA molecules. It was proposed at the time that this effect is caused by one particular type of MC adduct occurring in clusters at rare segments of the DNA. The present finding, implicating the relatively rare MC intrastrand cross-link to cause bending or increased flexibility, could explain the global conformational change described in this early report.

Significance. There is increasing evidence for the hypothesis that a critical function of many DNA-binding proteins is to bend DNA. This is supported, for example, by experiments showing that recombination or transcription was enhanced by replacing protein binding sequences with intrinsically bent DNA segments. (For a discussion and specific references, see ref 44.) Apparently related to this phenomenon, several drugs which bend DNA have been shown to *stimulate* binding of DNA-

binding proteins, perhaps by mimicking the protein-caused deformation of the DNA. Intriguing examples are the cisplatin intrastrand cross-link (*24, 25*) and BPDE−guanine adducts (*26*). Such activity of a drug may functionally contribute to its biological effects. The intrastrand cross-link of MC is identified here as a new member of the class of DNA-bending drug adducts, and thus it is a potential candidate for the above effects on protein binding. For example, since this lesion is formed specifically at GpG sequences, it is attractive to speculate that such effects might be observed in the case of the transcription factor, Sp1 protein, which recognizes the GpG-rich GC box (*45*). As an exciting precedent, adducts of the guanine-N^2-specific minor groove alkylator BPDE created strong artificial binding sites of Sp1 in fragments of DNA (*26*). However, the 15° DNA bending angle at the MC adduct **5**, while it is comparable to the mechlorethamine-caused bending [12.4−16.8° (*22*)], is smaller than that of adducts of cisplatin [40° for the intrastrand (*30*) and 45° for the interstrand adducts (*18*)]. Thus it may not be sufficient to give rise to similar activity. In any case, it will be of great interest to study the binding of Sp1 and other DNA-binding proteins to MC adduct-modified DNA in order to probe these possibilities.

Acknowledgment. This work was supported by NIH Grants GM32681 and GM45804 (P.B.H.) and CA28681 (M.T.), and a Research Centers in Minority Institutions award RR03037 from the Division of Research Resources, NIH (M.T.). We thank Ms. K. Bennett and Ms. S. Syrkett for assistance in preparation of the manuscript.

References

(1) Tomasz, M. (1994) The Mitomycins: Natural Cross-linkers of DNA. In *Molecular Aspects of Anti-Cancer Drug−DNA Interactions* (Neidle, S., and Waring, M. J., Eds.) Vol. 2, pp 312−349, CRC Press, Boca Raton, FL.

(2) Lown, J. W., and Majundar, K. C. (1977) Reactions of carzinophilin with DNA assayed by ethidium fluorescence assay. *Can. J. Biochem.* **55**, 630−636.

(3) Armstrong, R. W., Salvati, M. E., and Nguyen, M. (1992) Novel interstrand cross-links induced by the antitumor antibiotic carzinophyllin/azinomycin B. *J. Am. Chem. Soc.* **114**, 3144−3145.

(4) Tomasz, M., Lipman, R., Chowdary, D., Pawlak, J., Verdine, G. L., and Nakanishi, K. (1987) Isolation and structure of a covalent cross-link adduct between mitomycin C and DNA. *Science* **235**, 1204−1208.

(5) Tomasz, M., Chowdary, D., Lipman, R., Shimotakahara, S. Veiro, D., Walker, V., and Verdine, G. L. (1986) Reaction of DNA with chemically or enzymatically activated mitomycin C: Isolation and structure of the major covalent adduct. *Proc. Natl. Acad. Sci. U.S.A.* **83**, 6702−6706.

(6) Tomasz, M., Lipman, R., McGuinness, B. F., and Nakanishi, K. (1988) Isolation and characterization of a major adduct between mitomycin C and DNA. *J. Am. Chem. Soc.* **110**, 5892−5896.

(7) Bizanek, R., McGuinness, B. F., Nakanishi, K., and Tomasz, M. (1992) Isolation and structure of an intrastrand cross-link adduct of mitomycin C and DNA. *Biochemistry* **31**, 3084−3091.

(8) Bizanek, R., Chowdary, D., Arai, H., Kasai, M., Hughes, C. S., Sartorelli, A. C., Rockwell, S., and Tomasz, M. (1993) Adducts of mitomycin C and DNA in EMT6 mouse mammary tumor cells: Effects of hypoxia and dicumarol on adduct patterns. *Cancer Res.* **53**, 5127−5134.

(9) Li, V., and Kohn, H. (1991) Studies on the bonding specificity for mitomycin C-DNA monoalkylation processes. *J. Am. Chem. Soc.* **113**, 275−283.

(10) Kumar, S., Lipman, R., and Tomasz, M. (1992) Recognition of specific DNA sequences by mitomycin C for alkylation. *Biochemistry* **31**, 1399−1407.

(11) Kohn, H. Li, V.-S., and Tang, M. (1992) Recognition of mitomycin C−DNA monoadducts by UVRABC nuclease. *J. Am. Chem. Soc.* **114**, 5501−5509.

(12) Teng, S. P., Woodson, S. A., and Crothers, D. M. (1989) DNA sequence specificity of mitomycin cross-linking. *Biochemistry* **28**, 3901−3907.

(13) Millard, J. T., Weidner, M. F., Raucher, S., and Hopkins, P. B. (1990) Determination of the DNA cross-linking sequence specificity of reductively activated mitomycin C at single nucleotide resolution: Deoxyguanosine residues at CpG are cross-linked preferentially. *J. Am. Chem. Soc.* **112**, 3637−3641.

(14) Borowy-Borowski, H., Lipman, R., and Tomasz, M. (1990) Recognition between mitomycin C and specific DNA sequences for cross-link formation. *Biochemistry* **29**, 2999−3004.

(15) Toney, J. H., Donahue, B. A., Kellett, P. J., Bruhn, S. L., Essigmann, J. M., and Lippard, S. J. (1989) Isolation of cDNAs encoding a human protein that binds selectively to DNA modified by the anticancer drug cis-diamminedichloroplatinum (II). *Proc. Natl. Acad. Sci. U.S.A.* **86**, 8328−8332.

(16) Donahue, B. A., Augot, M., Bellon, S. F., Treiber, D. K., Toney, J. J., Lippard, S. J., and Essigmann, J. M. (1990) Characterization of a DNA damage-recognition protein from mammalian cells that binds specifically to intrastrand d(GpG) and d(ApG) DNA adducts of the anticancer drug cisplatin. *Biochemistry* **29**, 5872−5880.

(17) Brabec, V., Sip, M., and Leng, M. (1993) DNA conformational change produced by the site-specific interstrand cross-link of *trans*-diamminedichloroplatinum(II). *Biochemistry* **32**, 11676−11681.

(18) Sip, M., Schwartz, A., Vovelle, F., Ptak, M., and Leng, M. (1992) Distortions induced in DNA by cis-platinum interstrand adducts. *Biochemistry* **31**, 2508−2513.

(19) Lee, C.-S., Sun, D., Kizu, R., and Hurley, L. H. (1991) Determination of the structural features of (+)-CC-1065 that are responsible for bending and winding of DNA. *Chem. Res. Toxicol.* **4**, 203−213.

(20) Kizu, R., Draves, P., and Hurley, L. H. (1993) Correlation of DNA sequence specificity of anthramycin and tomaymycin with reaction kinetics and bending of DNA. *Biochemistry* **32**, 8712−8722.

(21) Xu, R., Mao, B., Xu, J., Li, B., Birke, S., Swenberg, C. E., and Geacintov, N. E. (1995) Stereochemistry-dependent bending in oligonucleotides by site-specific covalent benzo[a]pyrene diolepoxide−guanine lesions. *Nucleic Acids Res.* **23**, 2314−2319.

(22) Rink, S. M., and Hopkins, P. B. (1995) A mechlorethamine-induced DNA interstrand cross-link bends duplex DNA. *Biochemistry* **34**, 1439−1445.

(23) Bellon, S. F., and Lippard, S. J. (1990) Bending studies of DNA site-specifically modified by cisplatin, trans-diamminedichloroplatinum(II) and cis-$[Pt(NH_3)_2(N_3\text{-cytosine})Cl]^+$. *Biophys. Chem.* **35**, 179−188.

(24) Bruhn, S. L., Pil, P. M., Essigmann, J. M., Housman, D. E., and Lippard, S. J. (1992) Isolation and characterization of human cDNA clones encoding a high mobility group box protein that recognizes structural distortions to DNA caused by binding of the anticancer agent cisplatin. *Proc. Natl. Acad. Sci. U.S.A.* **89**, 2307−2311.

(25) Treiber, D. K., Zhai, X., Jantzen, H.-M., and Essigmann, J., (1994) Cisplatin−DNA adducts are molecular decoys for the ribosomal RNA transcription factor hUBF (human upstream binding factor). *Proc. Natl. Acad. Sci. U.S.A.* **91**, 5672−5676.

(26) McLeod, M., Powell, K. L., and Tran, N. (1995) Binding of the transcription factor, Sp1 to non-target sites in DNA modified by benzo[a]pyrene diolepoxide. *Carcinogenesis* **16**, 975−983.

(27) Sun, D. Y., and Hurley, L. H. (1994) Binding of Sp1 to the 21-bp repeat region of SV40 DNA: Effect of intrinsic and drug-induced DNA-bending between GC boxes. *Gene* **149**, 165−172.

(28) Kim, S. Y., and Rockwell, S. (1995) Cytotoxic potential of monoalkylation products between mitomycins and DNA: Studies of decarbamoyl mitomycin C in wild type and repair-deficient cell lines. *Oncol. Res.* **7**, 39−47.

(29) Basu, A. K., Hanrahan, C. J., Malia, S. A., Kumar, S., Bizanek, R., and Tomasz, M. (1993) Effect of site-specifically located mitomycin C−DNA monoadducts on in vitro DNA synthesis by DNA polymerases. *Biochemistry* **32**, 4708−4718.

(30) Rice, J. A., Crothers, D. M., Pinto, A. L., and Lippard, S. J. (1988) The major adduct of the antitumor drug cis-diamminedichloroplatinum(II) with DNA bends the duplex by approximately equal to 40 degrees toward the major groove. *Proc. Natl. Acad. Sci. U.S.A.* **85**, 4158−4161.

(31) Rink, S. M., Solomon, M. S., Taylor, M. J., Rajur, S. B., McLaughlin, L. W., and Hopkins, P. B. (1993) Covalent structure of a nitrogen mustard-induced DNA interstrand cross-link. *J. Am. Chem. Soc.* **115**, 2551−2557.

(32) Kumar, S., Johnson, W. S., and Tomasz, M. (1993) Orientation isomers of the mitomycin C interstrand cross-link in non-self-complementary DNA. Differential effect of the two isomers on restriction endonuclease cleavage at a nearby site. *Biochemistry* **32**, 1364−1372.

(33) Koo, H.-S., and Crothers, D. M. (1988) Calibration of DNA curvature and a unified description of sequence-directed binding. *Proc. Natl. Acad. Sci. U.S.A.* **85**, 1763−1767.

(34) Koo, H.-S., Wu, H.-M., and Crothers, D. M. (1986) DNA bending at adenine thymine tracts. *Nature* **320**, 501−506.

(35) Cornell, W. D., Cieplak, P., Bayly, C. I., Gould, I. R., Merz, K. M., Ferguson, D. M., Spellmeyer, D. C., Fox, T., Caldwell, J. W., and Kollman, P. A. (1995) A second generation force field for the simulation of proteins, nucleic acids, and organic molecules. *J. Am. Chem. Soc.* **117**, 5179−5197.

(36) von Kitzing, E. (1992) Modeling DNA structures. *Prog. Nucleic Acid Res. Mol. Biol.* **43**, 87−108.

(37) Norman, D., Live, D., Sastry, M., Lipman, R., Hingerty, B. E., Tomasz, M., Broyde, S., and Patel, D. J. (1990) NMR and computational characterization of mitomycin cross-linked to adjacent deoxyguanosines in the minor groove of the d(T-A-C-G-T-A) d(T-A-C-G-T-A) duplex. *Biochemistry* **29**, 2861−2876.

(38) Sastry, M., Fiala, R., Lipman, R., Tomasz, M., and Patel, D. J. (1995) Solution structure of the monoalkylated mitomycin C−DNA complex. *J. Mol. Biol.* **247**, 338−359.

(39) Rao, S. N., Singh, U. C., and Kollman, P. (1986) Conformations of the noncovalent and covalent complexes between mitomycins A and C and d(GCGCGCGCGC)2. *J. Am. Chem. Soc.* **108**, 2058−2068.

(40) Arora, S. K., Cox, M. B., and Arjunan, P. (1990) Structural, conformational and theoretical binding studies of antitumor antibiotic porfiromycin, a covalent binder of DNA, by X-ray, NMR, and molecular mechanics. *J. Med. Chem.* **33**, 3000−3008.

(41) Remers, W. A., Rao, S. N., Wunz, T. P., and Kollman, P. (1988) Conformations of complexes between mitomycins and decanucleotides. 3. Sequence specificity, binding at C-10, and mitomycin analogs. *J. Med. Chem.* **31**, 1612−1620.

(42) Verdine, G. L. (1986) Binding of Mitomycin C to a Dinucleoside Phosphate and DNA, Ph.D. Thesis, Columbia University, New York.

(43) Kaplan, D. J., and Tomasz, M. (1982) Altered physico-chemical properties of the deoxyribonucleic acid−mitomycin C complex. Evidence for a conformational change in deoxyribonucleic acid. *Biochemistry* **21**, 3006−3013.

(44) Strauss, J. K., and Maher, L. J. (1994) DNA bending by asymmetric phosphate neutralization. *Science* **266**, 1829−1834.

(45) Gidoni, D., Dynan, W. S., and Tjian, R. (1984) Multiple specific contacts between a mammalian transcription factor and its cognate promoters. *Nature* **312**, 409−413.

TX950156Q